

# Changing the universality class of the three-dimensional Edwards-Anderson spin-glass model by selective bond dilution

F. Romá<sup>1</sup>

<sup>1</sup>*Departamento de Física, Universidad Nacional de San Luis, Instituto de Física Aplicada (INFAP), Consejo Nacional de Investigaciones Científicas y Técnicas (CONICET), Chacabuco 917, D5700BWS San Luis, Argentina*  
(Dated: September 29, 2020)

The three-dimensional Edwards-Anderson spin-glass model present strong spatial heterogeneities well characterized by the called *backbone*, a magnetic structure that arises as a consequence of the properties of the ground state and the low-excitation levels of such a frustrated Ising system. Using extensive Monte Carlo simulations and finite size scaling, we study how these heterogeneities affect the phase transition of the model. Although, we do not detect any significant difference between the critical behavior displayed by the whole system and that observed inside and outside the backbone, surprisingly, a selective bond dilution of the complement of this magnetic structure induces a change of the universality class, whereas no change is noted when the backbone is fully diluted. This finding suggests that the region surrounding the backbone plays a more relevant role in determining the physical properties of the Edwards-Anderson spin-glass model than previously thought. Furthermore, we show that when a selective bond dilution changes the universality class of the phase transition, the ground state of the model does not undergo any change. The opposite case is also valid, i. e., a dilution that does not change the critical behavior significantly affects the fundamental level.

PACS numbers: 75.10.Nr, 75.40.Mg

Both, the singular phenomenology that glassy materials display and the enormous technical difficulties that must be overcome in order to study them, have promoted them as one of the central topics in modern physics. The most serious attempts to elucidate the physical origin of this behavior have led to the development of new highly sophisticated experimental, theoretical and simulation techniques. Although over the years this effort has paid off, it is still unclear how, under certain conditions relatively simple models are able to exhibit this phenomenon.

Typical glassy models have been studied countless times by performing increasingly powerful simulations that have allowed to characterize with greater precision some few aspects of the problem, but that have not been enough to get to the bottom of this matter. At present, however, studying the heterogeneities that characterize these complex systems seems to be a promising way to understand them a little more in depth [1].

These ideas apply to the case of the spin glasses, magnetic systems that have both quenched disorder and frustration [2, 3]. The paradigmatic Edwards-Anderson (EA) spin-glass model [4] present both spatial and nonequilibrium dynamical heterogeneities which are linked to each other [5–7]. These spatial heterogeneities are well characterized by a structure called *backbone* [8] which, in general, originates as a consequence of the properties of the ground state and the low-excitation levels of this system [9, 10]. Extensive simulations have shown that the nonequilibrium dynamic behavior displayed within the backbone differs qualitatively from what is observed outside of this structure. Such numerical results suggest that the separation of the system in two components (the backbone and its complement) is not trivial, so a suitable *backbone picture* could be essential to describe the physics of spin glasses.

Unfortunately, there are great difficulties to perform such calculations. On one hand, since the computation of ground state configurations of the three-dimensional (3D) EA model is a NP-hard problem, considerable numerical effort is required to calculate the backbone of a particular realization of the quenched disorder (sample). As a consequence, only a limited number of samples of small sizes can be calculated efficiently. On the other hand, although in average approximately 57% of bonds belong to the backbone and the rest to its complement, for a considerable number of samples these structures can have very different sizes, i. e., their size distributions are very broad [9]. In addition, both the backbone and its complement percolates (simultaneously), and are composed by a giant component and several finite clusters. These factors make it extremely difficult to determine which processes dominate physics within these regions.

In this work we focus on studying how these spatial heterogeneities affect the critical behavior of the 3D EA model. Using Monte Carlo simulations we calculate at equilibrium and for different lattice sizes, the correlation length and the spin-glass susceptibility for the whole system but also for the backbone and its complement. A finite size scaling study suggests that the critical behavior is unaffected by such heterogeneities. However, surprisingly, the universality class of the phase transition can be changed by a selective bond dilution: While no changes are observed when the backbone is completely diluted, in the opposite case in which the complement of this structure is removed we obtain a different set of critical exponents. This finding suggests that the region surrounding the backbone plays a more relevant role than previously thought and therefore we will call it the *glass* region. Furthermore, we show that when a selective bond dilution changes the universality class of the phase transition, the ground state of the system does not undergo any change. The opposite case

is also valid, i. e., a dilution that does not change the critical behavior significantly affects the fundamental level.

In the 3D EA spin-glass model [4], a set of  $N$  Ising spins  $\sigma_i = \pm 1$  are placed in a cubic lattice of linear dimension  $L$  ( $N = L^3$ ). Its Hamiltonian is

$$H = - \sum_{(i,j)} J_{ij} \sigma_i \sigma_j, \quad (1)$$

where  $(i,j)$  indicates a sum over the six nearest neighbors. The coupling constants or bonds,  $J_{ij}$ 's, are independent random variables drawn from a distribution with mean value zero and variance one. Here, we use a bimodal distribution, i.e.,  $J_{ij} = \pm 1$  with equal probability. In order to minimize finite-size effects we take periodic boundary conditions in all directions.

This model has a highly degenerate ground state [11, 12]. For a single sample it is possible to identify the so-called *rigid* bonds which do not change their state (satisfied or frustrated) in all its ground-state configurations [8]. Those bonds form the backbone while the complementary set, the *flexible* bonds, composes the glass region. Using the algorithm proposed in Ref. [9], we have calculated both structures for  $10^4$  samples for each size  $L = 4$  and  $L = 6$ ,  $10^3$  for  $L = 8$ , and 320 for  $L = 10$ . In addition, to calculate different observables at equilibrium we use a parallel tempering algorithm [13]. Details of the simulations are given in the Supplemental Material (SM).

At low temperatures spatial heterogeneities affect almost any observable. For example, Fig. 1 (a) shows the average energies per bond  $u$ ,  $u^B$ , and  $u^G$ , as function of temperature  $T$  for, respectively, the whole system, the backbone, and the glass, for samples of  $L = 10$ . Note that the curve of  $u^G$  display a minimum at approximately the critical temperature  $T_c = 1.1019(29)$  [14] and  $u^G > u > u^B$  for finite  $T$ , which evidence that the glass region concentrates the greatest frustration of the system. We indicate with arrows two particular points,  $a$  and  $b$ , to show that it is possible to have the same value of  $u^G$  at temperatures, respectively, below and above  $T_c$ , one of the reasons it was assumed (wrongly) that this region is in a paramagnetic phase for  $T > 0$  [9].

Unlike bonds separating the spins into groups may not be a trivial task. Typically two sets are chosen, the solidary spins which maintain their relative orientation in all configurations of the ground state and are connected by rigid bonds to each other, and the remaining ones that are called non-solidary spins. Although the backbone and the glass regions have roughly the same number of bonds, this separation produces two sets with very different fractions of spins: 77% and 23% of, respectively, solidary and non-solidary spins. Such a rule was chosen because, a priori, the backbone was considered the most important structure in the system.

Here, assuming both the backbone and glass are of equal importance, we use these structures to separate the spins in two groups. We call  $\Omega^B$  ( $\Omega^G$ ) to the set of spins connected to almost a rigid (flexible) bond, where the superscript  $B$  ( $G$ ) indicates that such region is dominated by the backbone (glass). Since some spins are connected to both rigid and flexible

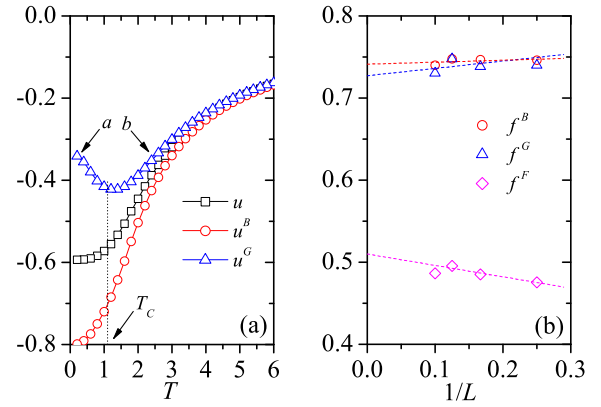


FIG. 1: (Color online) (a) Average energies per bond  $u$ ,  $u^B$ , and  $u^G$ , as function of  $T$ . Arrows indicate the critical temperature and two particular points on the  $u^G$  curve,  $a$  and  $b$ , located below and above  $T_c$ . (b) Average fractions of spins  $f^B$ ,  $f^G$ , and  $f^F$ , as function of  $1/L$ .

bonds these two sets intersect,  $\Omega^F = \Omega^B \cap \Omega^G$ , where now the superscript  $F$  denotes the frontier between these structures.

In Fig. 1 (b) we can see the average fractions of spins that belong to the sets  $\Omega^B$  ( $f^B$ ),  $\Omega^G$  ( $f^G$ ), and  $\Omega^F$  ( $f^F$ ), as function of  $1/L$ . In the thermodynamic limit these quantities tend approximately to  $f^B \sim 0.74$ ,  $f^G \sim 0.73$ , and  $f^F \sim 0.51$ , which shows that the mean numbers of spins in the backbone and glass regions are very similar, and the frontier has half of the spins of the system, i. e., both structures interpenetrates each other sharing a region whose size is proportional to  $N$ .

Having separated the spins in different sets as described above, it is possible to calculate other observables within each of these regions. In particular, to study the critical behavior of the 3D EA model, we calculate the correlation length  $\xi^x$  defined as [15] (in cases where a given quantity is not calculated over the whole system, we use a superscript  $x$  to indicate the region over which it is evaluated)

$$\xi^x = \frac{1}{2 \sin(|\mathbf{k}_{\min}|/2)} \left[ \frac{\chi^x(0)}{\chi^x(\mathbf{k}_{\min})} - 1 \right]^{1/2}, \quad (2)$$

where  $\mathbf{k}_{\min} = (2\pi/L, 0, 0)$  is the smaller nonzero wave vector and  $\chi^x(\mathbf{k})$  is the wave vector dependent spin-glass susceptibility,

$$\chi^x(\mathbf{k}) = \frac{1}{N_{\Omega^x}} \sum_{i,j \in \Omega^x} [(q_i q_j)_T]_{\text{av}} e^{i\mathbf{k} \cdot (\mathbf{r}_i - \mathbf{r}_j)}. \quad (3)$$

Here,  $q_i = \sigma_i^\alpha \sigma_i^\beta$  is the single spin overlap between two replicas of the system  $\alpha$  and  $\beta$ ,  $N_{\Omega^x}$  is the number of spins of region  $\Omega^x$ , and  $\mathbf{r}_i$  is the vector of position of the  $i$ -th spin.  $\langle \dots \rangle_T$  and  $[\dots]_{\text{av}}$  represent, respectively, the thermal and disorder averages. The correlation length divided by  $L$  is a dimensionless quantity which scales as [16]

$$\frac{\xi^x}{L} = \tilde{S}^x [L^{1/\nu^x} (T - T_c^x)/T_c^x], \quad (4)$$

where  $\tilde{S}^x$  is a universal scaling function,  $T_c^x$  is the critical temperature, and  $\nu^x$  is a critical exponent. If the system experiences a phase transition, according to Eq. (4) the curves of  $\xi^x/L$  for different lattice sizes should intersect at  $T_c^x$ .

Figure 2(a) shows the correlation length calculated for the whole system,  $\xi$ , for different lattice sizes as indicated. The curves intersect at approximately the true critical temperature and, using precise values of  $T_c = 1.1019(29)$  and  $\nu = 2.562(42)$  taken from recent literature [14], we obtain a good data collapse (see inset). This example shows that, despite the limitations of our calculations (performed for few samples of very small sizes), it is still possible to study the critical behavior of the model with a certain degree of accuracy.

Now, we focus on the backbone and glass regions. Figure 2(b) shows that the curves of  $\xi^B$  are very similar to those calculated for the whole system, and a good data collapse can be obtained using the same critical parameters as before (see inset). For the glass region, however, we do not obtain a result as robust as the previous one, see Fig. 2(c). Each pair of curves of  $\xi^G$  calculated for two consecutive sizes intersect at a temperature slightly higher than  $T_c$ , and their crossing point slowly moves towards lower temperatures as the system size increases. The scaling plot shows in the inset, performed again using  $T_c = 1.1019(29)$  and  $\nu = 2.562(42)$ , does not allow to achieve a good data collapse. This suggests that the results obtained for the glass region are probably affected by very strong finite-size effects.

In order to determine with certainty the universality class of a phase transition, it is necessary to analyze the scaling of a second observable that depends on an independent critical exponent. Therefore, we consider the spin-glass susceptibility for a given region,  $\chi^x \equiv \chi^x[\mathbf{k} = (0, 0, 0)]$ , and the corresponding critical exponent  $\eta^x$ . Although for the whole system and the backbone we have obtained good data collapses of the correlation length using a conventional scaling Eq. (4), for the susceptibility we choose an extended scaling scheme [17]

$$\chi^x = (LT)^{2-\eta^x} \tilde{C}^x[(LT)^{1/\nu^x} (1 - (T_c^x/T)^2)], \quad (5)$$

which is more appropriate for dealing with samples of small sizes. Using the critical parameters  $T_c = 1.1019(29)$ ,  $\nu = 2.562(42)$ , and  $\eta = -0.3900(36)$  [14], we obtain excellent data collapses for all regions, and in particular for the glass one (from now on and for reasons of space, the different curves of susceptibility and the corresponding scaling plots are shown in the SM). We conclude then that the critical behavior is the same in each of the regions in which we have divided the system.

The previous results seem to suggest that the spatial heterogeneities we are considering are not closely related to the critical behavior of this system. This conclusion, however, is not entirely accurate. As we shall see below, a selective bond dilution allows us to unveil surprising features of the backbone and glass regions, otherwise impossible to detect in a simulation that does not take into account such structures.

First, for comparison purposes, we calculate the correlation length and the spin-glass susceptibility for the 3D ran-

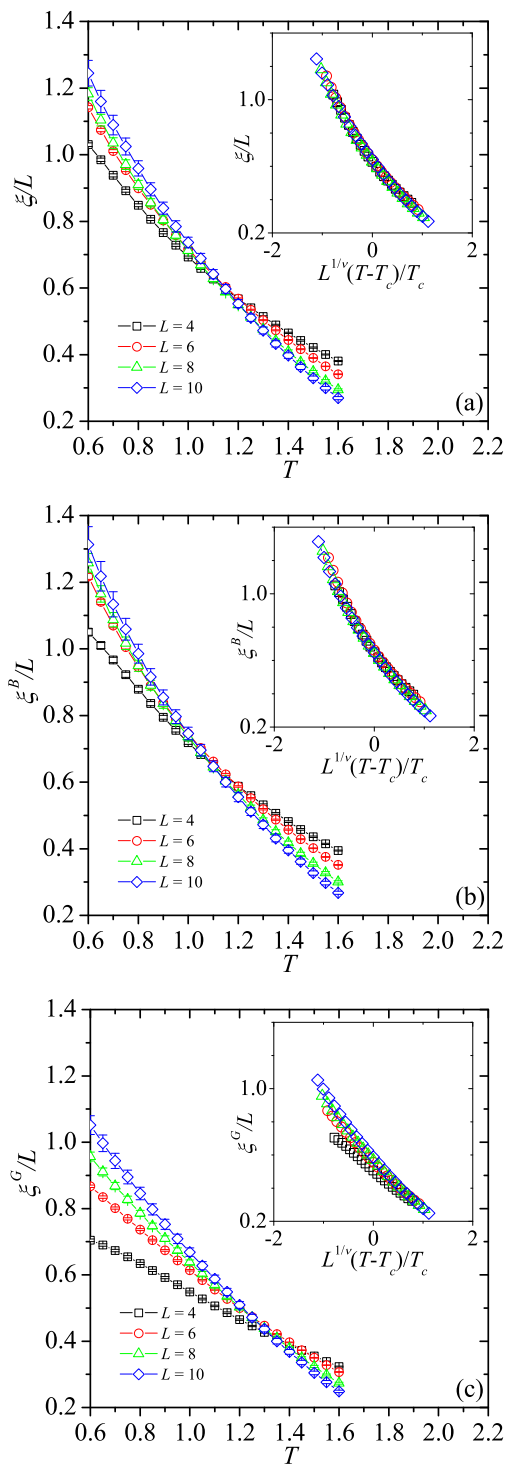


FIG. 2: (Color online) Correlation length function divided by  $L$  as function of  $T$  for (a) the whole system, and for (b) the backbone and (c) glass regions. Insets show the corresponding data collapses performed according to Eq. (4) using the critical parameters  $T_c = 1.1019(29)$  and  $\nu = 2.562(42)$  [14].

dom bond-diluted EA spin-glass model,  $\xi^*$  and  $\chi^*$ , respectively. We use the same lattice sizes and number of samples

as before, with 50% of dilution. In Fig. 3(a) we can observe that the curves of  $\xi^*/L$  cross at  $T_c^* = 0.75(1)$  and, using the critical exponents  $\nu = 2.562(42)$  and  $\eta = -0.3900(36)$ , good data collapses are obtained for this quantity (see inset) and for the spin-glass susceptibility (see SM). This numerical experiment corroborates something that is well known, that a random bond dilution does not change the universality class of the 3D EA spin-glass model [18].

Surprisingly, a selective bond dilution is capable of inducing a change of universality. Figure 3(b) shows the correlation length curves calculated for the backbone region,  $\xi^{B*}$ , obtained after diluting the entire glass region. On one hand, we observe a cross at  $T_c^{B*} = 2.02(1)$ , a critical temperature higher than that of the undiluted system. This is an expected result, since by removing the region with the greatest frustration of the system, the phase should be more stable in terms of energy and the critical temperature should rise. But, on the other hand, even more important is that we obtain two critical exponents,  $\nu^{B*} = 0.81(1)$  and  $\eta^{B*} = 0.47(1)$ , that are obviously very different from those of the 3D EA spin-glass model. These critical parameters were calculated by performing a careful statistical analysis of the data which is described in the SM. Using them, good data collapses are obtained for the correlation length [see inset in Fig. 3(b)] and for the corresponding spin-glass susceptibility,  $\chi^{B*}$  (see SM).

This phase transition probably belongs to the universality class of the 3D ferromagnetic Ising model. There are at least two reasons to suppose that this is so. Firstly, the backbone has very little frustration, i. e., approximately only 10% of its bonds are frustrated in the ground state [9]. In comparison, the ferromagnetic phase transition in the 3D Ising model persists even if a fraction of bonds up to 22% are randomly replaced by antiferromagnetic bonds, most of which contribute directly to the frustration of the fundamental level [19]. Therefore, these energetic considerations and also previous studies of the nonequilibrium dynamic of the 3D EA model [20], suggest that the backbone would be able of sustaining a ferromagnetic-like order.

Secondly, simulating the 3D ferromagnetic Ising model for small lattice sizes up to  $L = 10$ , we obtain a set of *effective* critical exponents,  $\nu_{\text{eff}}^I \approx 0.8$  and  $\eta_{\text{eff}}^I \approx 0.5$ , that differ from the values of this universality class,  $\nu^I \approx 0.684$  and  $\eta^I \approx 0.037$  [21], but which are similar to those calculated for the backbone,  $\nu^{B*} = 0.81(1)$  and  $\eta^{B*} = 0.47(1)$ . In addition, diluting 50% of the bonds of the 3D ferromagnetic Ising system at random, we determine that  $\nu_{\text{eff}}^{I*} \approx 0.9$  and  $\eta_{\text{eff}}^{I*} \approx 0.52$ . We conclude then that, having removed the glass region of the 3D EA model, the backbone undergoes a phase transition whose universality class probably belongs to the 3D Ising model but, since it is only possible to analyze lattices of small sizes, we cannot confirm that this is the case. Further studies should be performed to clarify this issue.

In the opposite case, when we dilute the backbone but keep the glass region, we observe in Fig. 3(c) that the correlation length curves,  $\xi^{G*}$ , intersect at  $T_c^{G*} = 0.64(2)$ . Unlike the previous case, this critical temperature is lower than

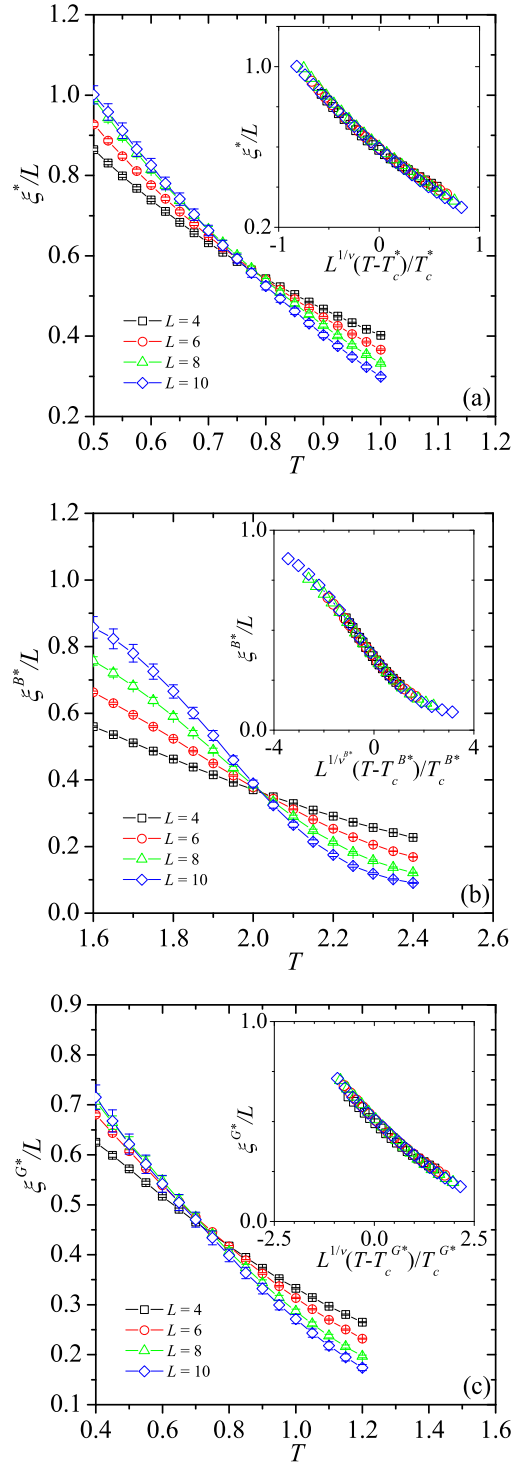


FIG. 3: (Color online) Correlation length function divided by  $L$  as function of  $T$  for a random bond dilution (a) of 50%, and for a selective bond dilution of (b) the glass and (c) backbone regions. Insets show the corresponding data collapses (see text).

$T_c$  since the most energetically stable region (backbone) has been removed. Using  $\nu = 2.562(42)$ , the inset shows a much better data collapse than that obtained in the undiluted case



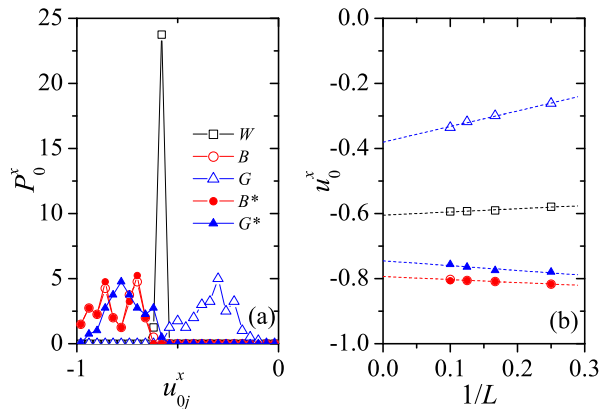


FIG. 4: (Color online) Probability distribution functions of ground-state energies per bond for samples of  $L = 10$ , and for the different regions as indicated. (b) Disorder average of these energies as function of  $1/L$ .

[Fig. 2(c)]. To confirm that this phase transition belong to the universality class of the 3D EA spin-glass model, we make a scaling plot of the susceptibility,  $\chi^{G^*}$ , using the exponent  $\eta = -0.3900(36)$ , which leads to a very good data collapse (see SM). In this way, it is justified that we have named this part of the system the glass region.

Finally, we observe that a selective bond dilution also affects other properties of the system, in particular its fundamental level. We calculate the probability distribution function,  $P_0^x$ , of ground-state energies per bond,  $u_{0j}^x$ , where as before the superscript  $x$  indicates the region over which this energy is evaluated and the conditions under which the calculations are performed (the undiluted and diluted cases). Figure 4(a) presents the distributions that were obtained for samples of  $L = 10$ , while the panel (b) shows the disorder average of each energy as function of  $1/L$ . Here, we can see important differences between the main regions of the system. In fact, a selective bond dilution of the glass region does not change the ground state of the backbone (the distributions of  $u_{0j}^B$  and  $u_{0j}^{B^*}$  are equals), while in the opposite case an appreciable effect is observed: the probability distributions of  $u_{0j}^G$  and  $u_{0j}^{G^*}$  are very different, and the latter overlaps appreciably with the corresponding one for the backbone. Therefore, a selective bond dilution can change the universality class of the phase transition of a given region leaving its ground state unchanged, and vice versa.

Summarizing, through an extensive analysis of the ground state of the 3D EA spin-glass model we have separated the lattice of the system in two components, the backbone and the glass. We show that the phase transitions observed within each of these regions have the same class of universality than that has the whole system, i. e., in the first instance the spatial heterogeneities seem not to affect the critical behavior of the model. However, diluting the glass we observe that the ground state of the backbone remain unchanged but, more importantly, we detect that the universality class of the phase

transition changes. In the opposite case, when the backbone is removed, we observe that the glass undergoes dramatic changes at its fundamental level, while the critical behavior remains the same as the undiluted system.

These results indicate that the critical behavior of the 3D EA spin-glass model originates from the interaction between two subsystems of very different nature, one of which dominates the other. The dilution process further reveals that there is no direct but subtle connection between the fundamental level of the system and this phenomenon. In fact, it is the non-trivial separation in backbone and glass, two structures defined in the ground state, that allows to unveil this phenomenon. Taking further advantage of these new elements could help improve current understanding of spin-glass systems.

I acknowledge financial support from CONICET (Argentina) under Project No. PIP 112-201301-00049-CO and Universidad Nacional de San Luis (Argentina) under Project No. PROICO P-31216.

- 
- [1] L. Berthier, G. Biroli, J.-P. Bouchaud, L. Cipelletti, and W. van Saarloos, *Dynamical Heterogeneities in Glasses, Colloids, and Granular Media* (Oxford Science Publishers, Oxford, 2011), Vol. 150.
  - [2] K. Binder and A.P. Young, *Rev. Mod. Phys.* **58**, 801 (1986).
  - [3] K. H. Fischer and J. A. Hertz, *Spin Glasses* (Cambridge University Press, Cambridge, 1991).
  - [4] S.F. Edwards and P.W. Anderson, *J. Phys. F* **5**, 965 (1975).
  - [5] F. Romá, S. Bustingorry, and P. M. Gleiser, *Phys. Rev. Lett.* **96**, 167205 (2006).
  - [6] F. Romá, S. Bustingorry, P. M. Gleiser, and D. Domínguez, *Phys. Rev. Lett.* **98**, 097203 (2007).
  - [7] F. Romá, S. Bustingorry, and P. M. Gleiser, *Eur. Phys. J. B* **89**, 259 (2016).
  - [8] F. Barahona, R. Maynard, and R. Rammal, *J. P. Uhry, J. Phys. A: Math. Gen.* **15**, 673 (1982).
  - [9] F. Romá, S. Risau-Gusman, A. J. Ramirez-Pastor, F. Nieto, and E. E. Vogel, *Phys. Rev. B* **82**, 214401 (2010).
  - [10] F. Romá and S. Risau-Gusman, *Phys. Rev. E* **88**, 042105 (2013).
  - [11] S. Kirkpatrick, *Phys. Rev. B* **16**, 4630 (1977).
  - [12] A. K. Hartmann, *Phys. Rev. E* **63**, 016106 (2000).
  - [13] K. Hukushima and K. Nemoto, *J. Phys. Soc. Jpn.* **65**, 1604 (1996).
  - [14] M. Baity-Jesi *et al.*, *Phys. Rev. B* **88**, 224416 (2013).
  - [15] M. Palassini and S. Caracciolo, *Phys. Rev. Lett.* **82**, 5128 (1999).
  - [16] H. G. Katzgraber, M. Körner, and A. P. Young, *Phys. Rev. B* **73**, 224432 (2006).
  - [17] I. A. Campbell, K. Hukushima, and H. Takayama, *Phys. Rev. Lett.* **97**, 117202 (2006).
  - [18] M. Hasenbusch, A. Pelissetto, and E. Vicari, *Phys. Rev. B* **78**, 214205 (2008).
  - [19] A. K. Hartmann, *Phys. Rev. B* **59**, 3617 (1999).
  - [20] F. Romá, S. Bustingorry, and P. M. Gleiser, *Phys. Rev. B* **81**, 104412 (2010).
  - [21] H. G. Ballesteros *et al.*, *Phys. Rev. B* **58**, 2740 (1998).

# Supplemental Material for: Changing the universality class of the three-dimensional Edwards-Anderson spin-glass model by selective bond dilution

F. Romá<sup>1</sup>

<sup>1</sup>*Departamento de Física, Universidad Nacional de San Luis, Instituto de Física Aplicada (INFAP),  
Consejo Nacional de Investigaciones Científicas y Técnicas (CONICET), Chacabuco 917, D5700BWS San Luis, Argentina*  
(Dated: September 29, 2020)

PACS numbers: 75.10.Nr, 75.40.Mg

## NUMERICAL SIMULATIONS

Monte Carlo simulations are performed using a parallel tempering algorithm [1, 2]. We use this technique to calculate both ground-state configurations [3, 4] and average values of different observables at equilibrium, for  $10^4$  samples for each size  $L = 4$  and  $L = 6$ ,  $10^3$  for  $L = 8$ , and 320 for  $L = 10$ .

This algorithm is implemented as follows. We simulate an ensemble of  $M$  noninteracting replicas of a system of  $N$  spins, each one associated to a different temperature in the interval  $[T_{min}, T_{max}]$  where, for simplicity, the difference between consecutive temperatures is chosen constant. A parallel tempering algorithm consists of two routines. One of them is a standard Monte Carlo procedure, i. e., an attempt to update a random selected spin of the ensemble (we randomly choose both a replica and a spin of this replica) with probability given by the Metropolis rule [5]. The second routine consists of an exchange of configurations between two replicas at consecutive temperatures which is attempted with the probability defined in Ref. [2]. The unit time (or step) of a parallel tempering algorithm consists of  $N \times M$  elementary steps of the standard Monte Carlo procedure, followed by a single trial of replica exchange.

The total simulation times (number of parallel tempering steps),  $t$ , required to equilibrate the system are chosen as  $t = 2 \times 10^5$  for  $L = 4$ ,  $t = 4 \times 10^5$  for  $L = 6$ ,  $t = 5 \times 10^5$  for  $L = 8$ , and  $t = 10^6$  for  $L = 10$ . We also use between  $M = 17$  and  $M = 21$  replicas of the system in each case. To reach equilibrium under a given condition  $x$  (the undiluted and diluted cases), it is necessary to choose that the highest temperature is above the critical one,  $T_{max} > T_c^x$ . In addition, once equilibrium is reached the average values of different observables are calculated over a time interval of the same length  $t$ .

Previously, it is necessary to find the backbone and glass regions of each realization of the quenched disorder. To determine which are the rigid and flexible bonds of a given sample, we use a very simple strategy [6, 7]:

1. A ground-state configuration  $C$  is calculated and its energy  $U_0$  is stored (to do so, we use a parallel tempering algorithm as explained in Ref. [4]).
2. Then, a bond  $J_{ij}$  of the sample is chosen at random.
3. The system being in configuration  $C$ , one of the spins

joined by the bond  $J_{ij}$ , i.e. either  $\sigma_i$  or  $\sigma_j$ , is flipped. This flip changes the “condition” of the bond from satisfied to frustrated, or vice versa.

4. The orientations of the spins  $i$  and  $j$  are frozen and, for this “constrained” system, a new ground-state configuration  $C'$  of energy  $U'_0$  is calculated.
5. If  $U'_0 > U_0$ , it follows that  $J_{ij}$  is a rigid bond (since we verify that there does not exist a ground-state configuration of energy  $U_0$  in which this bond appears with its changed condition).
6. If  $U' = U$ , then  $J_{ij}$  is a flexible bond (we find a ground-state configuration of energy  $U_0$  in which this bond appears with its changed condition; this configuration could have been found by exhaustively exploring the fundamental level of the unconstrained system).
7. The bond  $J_{ij}$  is added to the list of “checked” bonds, and the restrictions over the spins  $\sigma_i$  or  $\sigma_j$  are lifted.
8. If there are still non-checked bonds, a new bond  $J_{ij}$  is chosen among them and the process is repeated from step 3.

Ground-state configurations were calculated with the same parallel tempering algorithm as before, using the parameters given in Refs. [4, 7].

## SPIN-GLASS SUSCEPTIBILITY

In this section we present the spin-glass susceptibility curves for the different cases studied.

The spin-glass susceptibility is defined as

$$\chi^x = \frac{1}{N\Omega^x} \sum_{i,j \in \Omega^x} [\langle q_i q_j \rangle_T]_{av}. \quad (1)$$

Figures S1 (a), (b), and (c), show this quantity as function of  $T$  for, respectively, the whole system, i. e., the three-dimensional (3D) Edwards-Anderson (EA) model, and for its backbone and glass regions, for different lattice sizes as indicated. For all cases, we obtain excellent data collapses (see insets) using the critical parameters  $T_c = 1.1019(29)$ ,

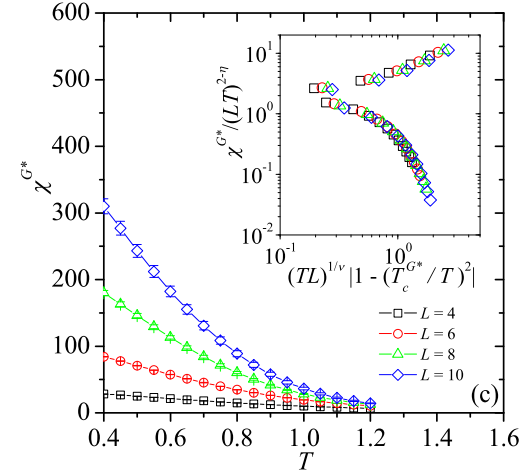
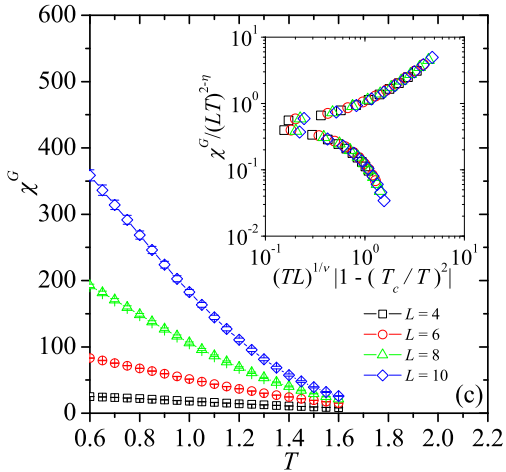
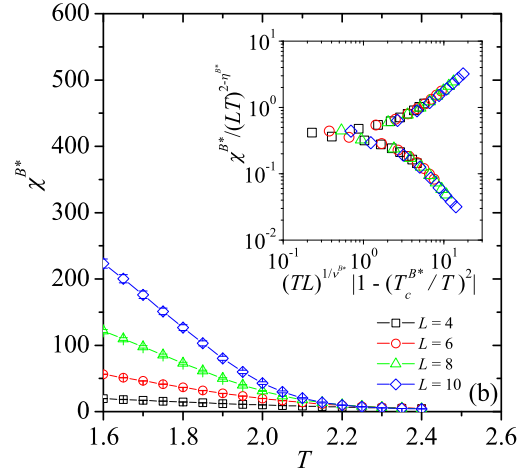
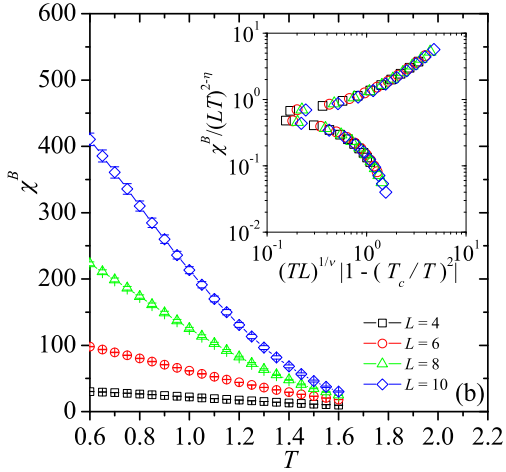
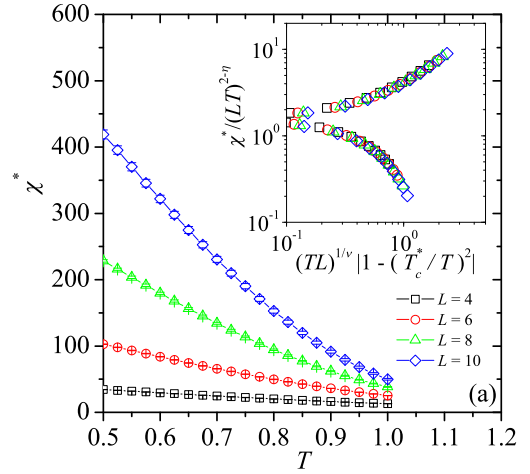
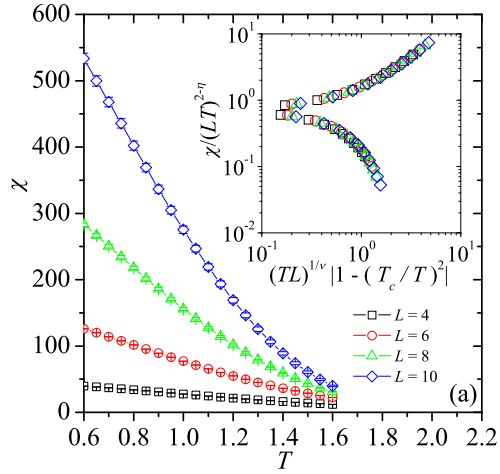


FIG. S1: (Color online) Spin-glass susceptibility as function of  $T$  for (a) the whole system, and for (b) the backbone and (c) glass regions. Insets show the corresponding data collapses (see text).

FIG. S2: (Color online) Spin-glass susceptibility as function of  $T$  for a random bond dilution (a) of 50%, and for a selective bond dilution of (b) the glass and (c) backbone regions. Insets show the corresponding data collapses (see text).

$\nu = 2.562(42)$ , and  $\eta = -0.3900(36)$  [8], and an extended scaling scheme [9]

$$\chi^x = (LT)^{2-\eta} \tilde{C}^x [(LT)^{1/\nu^x} (1 - (T_c^x/T^x)^2)]. \quad (2)$$

In Fig. S2 (a) we show the spin-glass susceptibility for the 3D random bond-diluted EA spin-glass model for a dilution of 50%. Instead, Figs. S2 (b) and (c) present, respectively, the

susceptibility calculated for the backbone region after diluting the entire glass region, and for the opposite case, when we dilute the backbone but keep the glass region. In the insets of panels (a) and (c) we show the data collapses obtained using the critical parameters  $\nu = 2.562(42)$  and  $\eta = -0.3900(36)$  [8], and the corresponding critical temperatures. Instead, for the isolated backbone, panel (b) shows that a good scaling plot is obtained if we use a different set of critical exponents,  $\nu^{B*} = 0.81(1)$  and  $\eta^{B*} = 0.47(1)$ , and  $T_c^{B*} = 2.02(1)$ . These last critical parameters were calculated as it is detailed in the next section.

### STATISTICAL ANALYSIS OF THE DATA

After a selective dilution of the glass region, we observe that the backbone undergoes a phase transition that does not belong to the universality class of the 3D EA spin-glass model. In fact, a scaling plot of both the correlation length  $\xi^{B*}$  and the spin-glass susceptibility  $\chi^{B*}$  using the critical exponents  $\nu = 2.562(42)$  and  $\eta = -0.3900(36)$ , leads to bad data collapses of these quantities.

To determine a suitable set of critical parameters  $T_c^{B*}$ ,  $\nu^{B*}$ , and  $\eta^{B*}$ , we use a procedure similar to that reported in Refs. [10, 11]. First, we fit each curve of correlation length and susceptibility to a fifth-order polynomial and, from now on, we work exclusively with these continuous functions. Then, we calculate  $T_c^{B*}$  and  $\nu^{B*}$  looking for the values of these parameters that allow us to achieve the best data collapse of the correlation length curves using a conventional scaling

$$\frac{\xi^{B*}}{L} = \tilde{S}^{B*} [L^{1/\nu^{B*}} (T - T_c^{B*}) / T_c^{B*}]. \quad (3)$$

In addition, to determine  $\eta^{B*}$ , we fix  $T_c^{B*}$  and  $\nu^{B*}$  to the values obtained previously and we follow a similar procedure for the spin-glass susceptibility, i. e., we look for the best data collapse of these curves but now using an extended scaling, Eq. (2). Finally, we calculate error bars on these critical parameters through a bootstrap method as described in Ref. [10].

- 
- [1] C. Geyer, *Computing Science and Statistics: Proceedings of the 23rd Symposium on the Interface* (American Statistical Association, New York, 1991), p. 156.
  - [2] K. Hukushima and K. Nemoto, *J. Phys. Soc. Jpn.* **65**, 1604 (1996).
  - [3] J. L. Moreno, H. G. Katzgraber, and A. K. Hartmann, *Int. J. Mod. Phys. C* **14**, 285 (2003).
  - [4] F. Romá, S. Risau-Gusman, A. J. Ramirez-Pastor, F. Nieto, and E. E. Vogel, *Physica A* **388**, 2821 (2009).
  - [5] N. Metropolis, A. W. Rosenbluth, N. M. Rosenbluth, A. H. Teller, and E. Teller, *J. Chem. Phys.* **21**, 1087 (1953).
  - [6] A. J. Ramirez-Pastor, F. Romá, F. Nieto, and E. E. Vogel, *Physica A* **336**, 454 (2004).
  - [7] F. Romá, S. Risau-Gusman, A. J. Ramirez-Pastor, F. Nieto, and E. E. Vogel, *Phys. Rev. B* **82**, 214401 (2010).
  - [8] M. Baity-Jesi *et al.*, *Phys. Rev. B* **88**, 224416 (2013).
  - [9] I. A. Campbell, K. Hukushima, and H. Takayama, *Phys. Rev. Lett.* **97**, 117202 (2006).
  - [10] H. G. Katzgraber, M. Körner, and A. P. Young, *Phys. Rev. B* **73**, 224432 (2006).
  - [11] D. A. Matoz-Fernandez and F. Romá, *Phys. Rev. B* **94**, 024201 (2016).